# GM2/GD2 and GM3 gangliosides have no effect on cellular cholesterol pools or turnover in normal or NPC1 mice

**Hao Li,* Stephen D. Turley,* Benny Liu,* Joyce J. Repa,*,† and John M. Dietschy[1,*]**

Departments of Internal Medicine* and Physiology,† University of Texas Southwestern Medical School, Dallas, TX 75390-9151

**Abstract** **These studies investigated the role of gangliosides in governing the steady-state concentration and turnover of unesterified cholesterol in normal tissues and in those of mice carrying the NPC1 mutation. In animals lacking either GM2/GD2 or GM3 synthase, tissue cholesterol concentrations and synthesis rates were normal in nearly all organs, and whole-animal sterol pools and turnover also were not different from control animals. Mice lacking both synthases, however, had small elevations in cholesterol concentrations in several organs, and the whole-animal cholesterol pool was marginally elevated. None of these three groups, however, had changes in any parameter of cholesterol homeostasis in the major regions of the central nervous system. When either the GM2/GD2 or GM3 synthase activity was deleted in mice lacking NPC1 function, the clinical phenotype was not changed, but lifespan was shortened. However, the abnormal cholesterol accumulation seen in the tissues of the NPC1 mouse was unaffected by loss of either synthase, and clinical and molecular markers of hepatic and cerebellar disease also were unchanged. These studies demonstrate that hydrophobic interactions between cholesterol and various gangliosides do not play an important role in determining cellular cholesterol concentrations in the normal animal or in the mouse with the NPC1 mutation.**—Li, H., S. D. Turley, B. Liu, J. J. Repa, and J. M. Dietschy. **GM2/GD2 and GM3 gangliosides have no effect on cellular cholesterol pools or turnover in normal or NPC1 mice.** ***J. Lipid Res.*** **2008.** 49: **1816–1828.**

**Supplementary key words** Niemann-Pick type C disease • membrane cholesterol • glycosphingolipids • neurodegeneration • cholesterol synthesis • brain cholesterol

Two of the most poorly understood regulatory processes in the body are the mechanism by which cells control the concentration of cholesterol in their plasma membrane and the reason why this sterol is constantly turned over. The higher the metabolic rate of a particular animal, the greater is the percentage of this membrane cholesterol pool that is renewed each day (1). To meet this apparently essential need to "turn over" the sterol component of the plasma membrane, virtually every cell invests in the elaborate machinery necessary to synthesize cholesterol de novo from acetyl CoA (1, 2). In addition, smaller amounts of cholesterol are also acquired from the outside through the receptor-mediated and bulk-phase uptake of lipoproteins containing the ligands apolipoprotein B-100 (apoB-100) or apoE (3–5). This newly synthesized and preformed cholesterol is then transported to the plasma membrane while an identical amount of sterol is removed from the outer membrane leaflet, transported to the liver, and excreted from the body (6). In this manner, there is constant turnover of sterol, but the concentration of unesterified cholesterol in every organ, and in the whole animal, remains remarkably constant at a characteristic value throughout life.

During transit through the plasma membrane, however, the cholesterol molecules undergo complex interactions with other lipids making up the two leaflets of the membrane. Although cholesterol itself is relatively uniformly distributed between both leaflets, other amphipathic lipids like phosphatidylethanolamine and phosphatidylserine are found principally in the inner (cytoplasmic) leaflet, whereas phosphatidylcholine and sphingomyelin are found largely in the outer leaflet. This asymmetry is even more striking with more-hydrophilic amphipathic molecules like glycolipids and, particularly, gangliosides that are almost exclusively localized in the outer leaflet. Furthermore, within the membrane itself, there is also regional organization, in that groups of molecules such as

*This work was supported by US Public Health Service Research Grant R01 HL-09610 (J.M.D., S.D.T.) and by grants from the Moss Heart Fund (J.M.D.) and The Ara Parseghian Medical Research Foundation (J.J.R.). Dr. Benny Liu also received post-doctoral support from the Ara Parseghian Medical Research Foundation and Dana's Angels Research Trust.*

*Manuscript received 14 April 2008.*

*Published, JLR Papers in Press, April 30, 2008.*
*DOI 10.1194/jlr.M800180-JLR200*

Abbreviations: CNS, central nervous system; NPC, Niemann-Pick type C.

[1] To whom correspondence should be addressed.
e-mail: john.dietschy@utsouthwestern.edu

cholesterol, sphingomyelin, glycolipids, and gangliosides cluster together through tight, lateral hydrophobic bonding to form microdomains or "rafts," in which are embedded glycosylphosphatidylinositol-anchored proteins (7–10). Such hydrophobic interactions may explain, in part, the forces dictating a particular concentration of sterol in the plasma membrane or in other compartments of the cell. For example, treatment of the outer surface of cultured cells with sphingomyelinase reduces hydrophobic bonding and causes part of the plasma membrane pool of cholesterol to collapse back into the metabolically active pool in the cytosol, where it suppresses cholesterol synthesis and is incorporated into the storage pool of cholesteryl esters (11, 12). On the other hand, when the potential for hydrophobic bonding increases in the late endosomal/lysosomal compartment of cells, as occurs in some of the lysosomal storage diseases, there is redistribution of cholesterol into that compartment (13–15).

Of the various glycosphingolipids present in the outer leaflet of the plasma membrane, gangliosides are the most complex. These compounds are present in the plasma membranes of most cells in small amounts, but are much more abundant on the cells of the central nervous system (CNS). These molecules apparently function by interacting with a variety of receptors and signal transducers involved in both cell signaling and adhesion (9, 16). There is currently little information, however, on how these complex molecules interact with sterol and so might alter cellular cholesterol homeostasis. Studies to elucidate such interactions have become feasible with the development of two knockout mouse strains. In the first of these models, the activity of the enzyme GM2/GD2 synthase, encoded by the gene *Galgt1*, was deleted (17). As seen in **Fig. 1**, this glycosyltransferase plays a critical role in the synthesis of many complex gangliosides, including those in the GA2 (*O*), GM2 (a), and GD2 (b) series. In the second mouse model, activity of the enzyme GM3 synthase, encoded by the gene *Siat9*, was deleted (18). This sialyltransferase is responsible for the synthesis of the GM3, GD3, and related gangliosides (Fig. 1). The *Galgt1*$^{-/-}$ mice have principally GM3 and GD3 gangliosides in their brain, whereas the *Siat9*$^{-/-}$ animals have predominantly gangliosides of the *O* series. In both models, early development and gross neurological function are normal (19).

In the current studies, these knockout models were utilized to explore two general areas related to the role of gangliosides in determining tissue cholesterol homeostasis. The first set of studies explored the effects of deleting the activity of GM2/GD2 synthase, GM3 synthase, or both synthases on tissue cholesterol concentrations, tissue cholesterol synthesis rates, and whole-animal sterol turnover kinetics. These studies focused particularly on measuring these parameters in different regions of the CNS. In the second group of experiments, these genetic deletions were bred into a mouse model of Niemann-Pick type C (NPC) disease in order to explore the role of various gangliosides

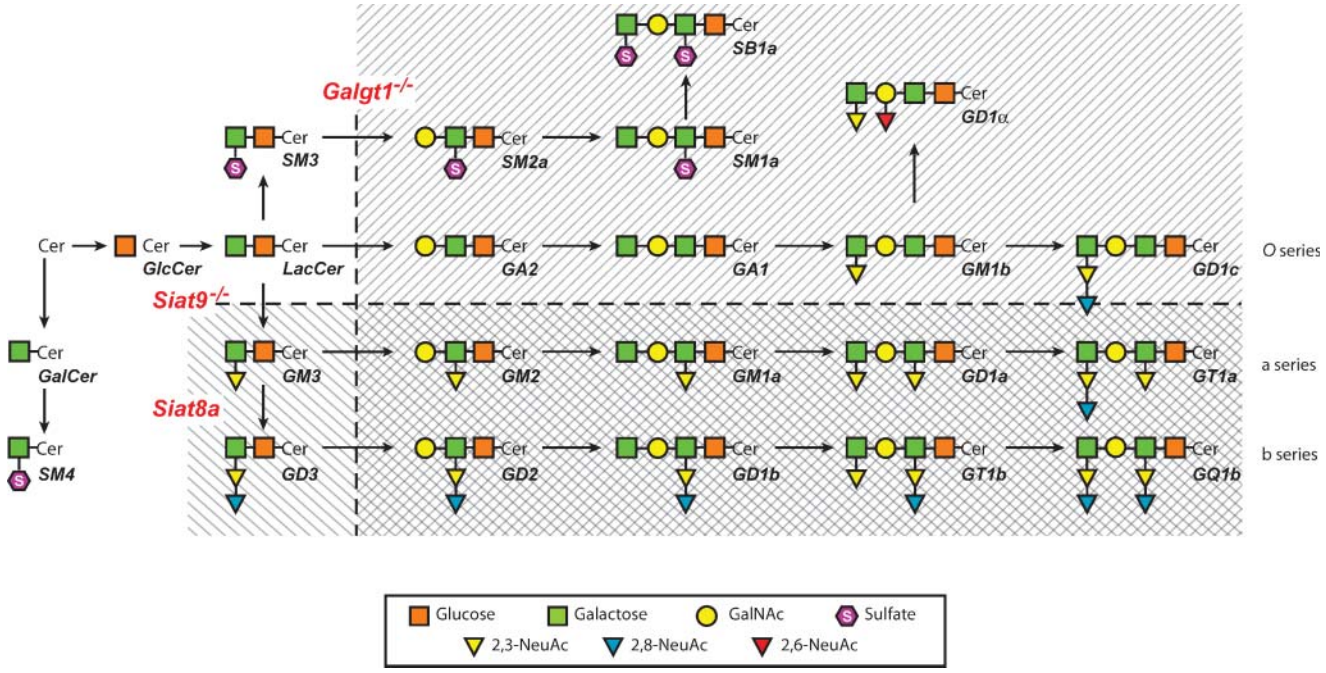


**Fig. 1.** Scheme showing the pathways for the synthesis of the major gangliosides. The genes encoding three critical enzymes are shown in red and represent GM2/GD2 synthase (*Galgt1*), GM3 synthase (*Siat9*), and GD3 synthase (*Siat8a*). The products not synthesized when *Galgt1* is inactivated are shown by the hatch marks sloping down to the left, and those not synthesized when *Siat9* is inactivated are shown by the hatch marks sloping down to the right. When both genes are inactivated, only the few glycolipids shown in the unhatched area are synthesized. The abbreviations represent ceramide (Cer), *N*-acetylgalactosamine (GalNAc), and *N*-acetylneuraminic acid (NeuAc). This diagram was developed by Dr. Richard Proia and was redrawn and modified slightly from reference (19) with permission of the authors and journal.

in affecting the abnormal distribution of cholesterol, and the serious hepatic and neurological phenotypes, seen in this genetic disease. Taken together, these studies provide the first systematic appraisal of how ganglioside and cholesterol metabolism may be linked and might together play roles in certain neurological diseases.

## MATERIALS AND METHODS

### Animals and diets

These studies were undertaken using ten different groups of genetically modified mice. Animals lacking NPC1 (*npc1*) function were obtained more than ten years ago from Dr. Peter G. Pentchev at the National Institutes of Health (20, 21), and mice lacking either GM2/GD2 (*Galgt1*) or GM3 (*Siat9*) synthase were provided four years ago by Dr. Richard L. Proia, also at the National Institutes of Health (17–19). The NPC1 mice obtained from the Pentchev laboratory were on a pure BALB/c background and, subsequently, were bred into a mixed 129/Sv and C57BL/6 background, which was similar to that present in the GM2/GD2 and GM3 knockout animals provided by Dr. Proia. These founding animals were used to establish large breeding colonies in the animal facility at The University of Texas Southwestern Medical School. These various stocks of animals were used, in turn, to generate groups of littermates that were normal controls (designated $Galgt1^{+/+}/Siat9^{+/+}$), lacked GM2/GD2 synthase activity ($Galgt1^{-/-}/Siat9^{+/+}$), lacked GM3 synthase activity ($Galgt1^{+/+}/Siat9^{-/-}$), or lacked both of these synthases ($Galgt1^{-/-}/Siat9^{-/-}$). In other studies, the mice lacking GM2/GD2 synthase were bred with animals lacking NPC1 function to yield littermates that were normal controls ($npc1^{+/+}/Galgt1^{+/+}$), lacked NPC1 function ($npc1^{-/-}/Galgt1^{+/+}$), or lacked both NPC1 and GM2/GD2 synthase functions ($npc1^{-/-}/Galgt1^{-/-}$). Similar animals were generated that were normal controls ($npc1^{+/+}/Siat9^{+/+}$), lacked NPC1 function ($npc1^{-/-}/Siat9^{+/+}$), or lacked both NPC1 and GM3 synthase activity ($npc1^{-/-}/Siat9^{-/-}$). The NPC1 and GM3 animals were genotyped utilizing protocols described elsewhere (18, 20). The GM2 mice were genotyped using a protocol outlined on the Mutant Mouse Regional Resource Center's website, together with instructions provided by Dr. Proia's laboratory (22).

All of these groups of animals were kept in the same facility under conditions of controlled temperature and alternate 12 h periods of light and darkness. They were maintained in plastic colony cages and, after weaning at 19–20 days of age, were allowed access to a low-cholesterol (0.02%, w/w) pelleted rodent diet (no. 7001, Harlan Teklad). In one study, additional cholesterol (1.0%, w/w) was added to a powdered form of this same diet and fed from the time of weaning. All experiments were carried out on animals 49 ± 1 days of age, using males and females, as designated in the legend to each figure. Tissues were harvested at the end of the dark cycle, when the mice were in the postprandial state.

In one experiment, the age at death was recorded in some groups of animals lacking NPC1 function or that were deficient in both NPC1 and GM3 synthase activities. The general clinical condition of these mice was monitored daily. Once the mice began to show difficulty accessing the pelleted low-cholesterol diet, they were also provided access to a powdered form of this diet. When the mice were no longer able to take food or water, they were humanely euthanized, and this was considered the day of death.

### Tissue sampling

At the termination of the various experiments, all mice were dissected in a standardized manner and all organs were weighed. The residual carcass, containing predominantly skin, skeleton, marrow, and muscle, was also weighed and processed. In most experiments, the entire CNS was removed, weighed, and processed. In other experiments, the CNS was dissected in a standardized manner into cerebrum, cerebellum, mid-brain, brain stem, and spinal cord before being weighed and processed. Because every tissue was weighed and processed, the values for cholesterol content and synthesis in all organs could be summed to give whole-animal values.

### Plasma and tissue lipid concentrations

Blood was drawn from the inferior vena cava and anticoagulated with heparin at the termination of the experiments. Plasma total cholesterol and triacylglycerol concentrations were measured as previously described (23, 24). Aliquots of every tissue were saponified, and the cholesterol was extracted and quantified utilizing gas chromatography (23). The plasma lipid concentrations are expressed as milligrams/deciliter, and the tissue cholesterol levels are expressed as milligrams of cholesterol found per gram wet weight of tissue (mg/g).

### Rates of cholesterol synthesis in each organ

The rates of cholesterol synthesis in all of the tissues were measured in vivo as previously described (25). Each animal was administered a bolus of $^3H_2O$ and euthanized 1 h later. The amount of $^3H$ incorporated into sterols was then determined, and these rates of cholesterol synthesis are expressed as nanomoles of $^3H_2O$ incorporated into sterols per hour per gram wet weight of tissue (nmol/h/g).

### Neuromuscular coordination

In one experiment, a measure of neuromuscular coordination was carried out in three genetically altered groups of mice. The accelerating rotarod apparatus (Rotamex 4/8; Columbus Instruments, Columbus, OH) was used to measure motor coordination (26). Each mouse was placed on the rotating rod at a starting speed of 4 rpm, and this speed was gradually increased to 40 rpm by 10 min. Four trials were carried out each day, with a rest period of 1 h between the first two trials and the last two trials. These data are reported as the seconds the animal remained on the apparatus.

### Determination of relative mRNA levels

Quantitative real-time (qRT)-PCR was performed using an Applied Biosystems 7900HT sequence detection system and SYBR-green chemistry (27). Total RNA was isolated from the whole cerebellum using RNA STAT-60 (Tel-Test), and 2 μg of total RNA was treated with RNase-free DNase (Roche Diagnostics), then reverse-transcribed with random hexamers using SuperScript II (Invitrogen). Gene-specific primers were designed using Primer Express Software (Perkin Elmer) and validated by analysis of template titration and dissociation curves (28). Primer sequences are provided elsewhere (26). Ten microliters of qRT-PCR reaction volumes contained 25 ng of reverse-transcribed RNA, each primer (150 nM), and 5 μl of 2× SYBR-green PCR master mix (Applied Biosystems). The values for these mRNA levels were calculated by the comparative cycle number determined at threshold ($C_T$) method (user Bulletin no. 2, Perkin Elmer) using cyclophilin as the invariant control gene. Values are presented relative to the levels found in the control mice, which were arbitrarily set at 1.0.

### Liver function tests

In one study, plasma was sent to a commercial laboratory for determination of the liver function tests alkaline phosphatase,

aspartate aminotransferase, and alanine aminotransferase. These data are presented as units per liter of plasma (U/l).

### Calculations

Tissue cholesterol concentrations and synthesis rates are presented per gram wet weight of tissue. When multiplied by organ weights and summed, these values give the whole-animal cholesterol content and rate of cholesterol synthesis. These values were then normalized to a constant body weight of 1 kg to give whole-animal cholesterol pools, expressed as milligrams per kilogram body weight (mg/kg), and whole-animal synthesis rates, expressed as nanomoles of $^3H_2O$ incorporated into sterols per day per kilogram body weight. These latter values were then converted to whole-animal cholesterol synthesis rates expressed as milligrams of cholesterol synthesized per day per kilogram body weight (mg/day/kg), knowing that 1.45 atoms of carbon are incorporated into the sterol molecule per 1.00 atoms of $^3H$ from $^3H_2O$ (29, 30). All of the data are presented as means ± SEM for the number of animals indicated in the figure legends. Differences between these mean values in Figs. 2–5 were tested for statistical significance ($P < 0.05$) using a 2-tailed unpaired Student's *t*-test (Graph-Pad Software, Inc.; San Diego, CA). Significant differences are indicated by an asterisk (*). In Figs. 7–9, one-way ANOVA, followed by the Newman-Keuls multiple comparison test, was used for analysis of the data, and significant differences in the groups are designated with different letters. Significant differences in survival curves (Fig. 6) were determined by Wilcoxon-Gehar and log-rank analyses.

## RESULTS

These studies were all carried out in young adult mice 49 ± 1 days of age. The flux of cholesterol across the organs of such animals has been well characterized (21, 31) and, at this age, the *npc1*$^{-/-}$ mice were in relatively good health and without gross neurological deficits (26). Control *Galgt1*$^{+/+}$/*Siat9*$^{+/+}$ mice were derived from the littermates of the three groups of knockout mice; however, no differences in cholesterol metabolism were found in the control animals derived from these three sources, so that data from these animals have been combined in **Fig. 2** into a single group designated *Galgt1*$^{+/+}$/*Siat9*$^{+/+}$. As previously established, the *Galgt1*$^{-/-}$/*Siat9*$^{+/+}$ animals lacked GM2/GD2 and more complex, related gangliosides in the brain, whereas the *Galgt1*$^{+/+}$/*Siat9*$^{-/-}$ animals lacked GM3 and related gangliosides (18, 19, 32). Although some of these animals were reported to have subtle abnormalities in the CNS (18, 32), early development and growth were normal. This was also found to be the case in the present study, where the weights of the 49 day-old *Galgt1*$^{-/-}$/*Siat9*$^{+/+}$ (24 ± 1 g) and *Galgt1*$^{+/+}$/*Siat9*$^{-/-}$ (26 ± 1 g) mice were nearly the same as the control animals (26 ± 1 g) (Fig. 2A). In contrast, the *Galgt1*$^{-/-}$/*Siat9*$^{-/-}$ animals, which lacked all complex gangliosides of the GM2/GD2 and GM3 series (Fig. 1) were reported to develop poorly and die at an early age (19). This also was found to be the case in the present study, where nearly two-thirds of the animals died before the age of 49 days. Consequently, these studies were carried out on the survivors, and these animals had a significantly lower body weight (16 ± 1 g) than the other three groups at 49 days of age (Fig. 2A). The plasma total cholesterol and triacylglycerol levels were also similar in the control and single-knockout animals, but the plasma cholesterol was slightly elevated and the

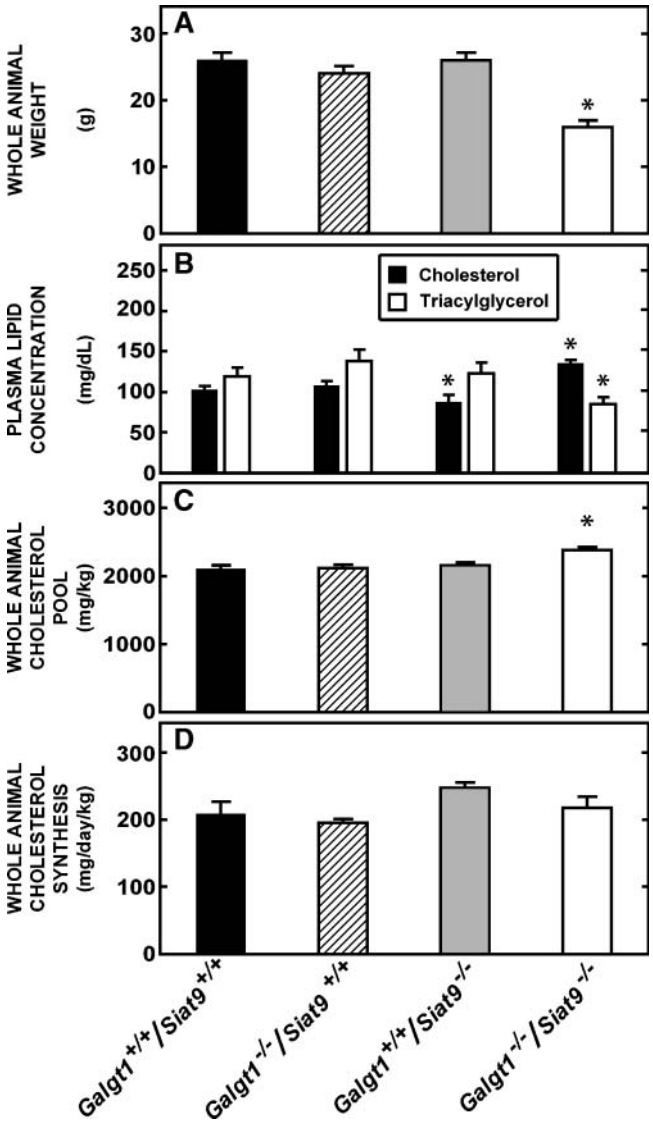


**Fig. 2.** Whole-animal weights, cholesterol pools, and synthesis rates in the various knockout animals. All mice in these groups were males, 49 days of age. A: Animal weights at the time the studies were undertaken in the *Galgt1*$^{+/+}$/*Siat9*$^{+/+}$ (n = 11), *Galgt1*$^{-/-}$/*Siat9*$^{+/+}$ (n = 6), *Galgt1*$^{+/+}$/*Siat9*$^{-/-}$ (n = 10), and *Galgt1*$^{-/-}$/*Siat9*$^{-/-}$ (n = 6) mice. B: Plasma cholesterol and triacylglycerol levels in these animals. After determining the cholesterol content of all tissues in the body, the values were summed and normalized to a body weight of 1.0 kg. These values are presented in C as milligrams of cholesterol present in the whole animal per kilogram body weight. Similarly, the rates of synthesis in all organs were summed and normalized to a 1.0 kg body weight. These $^3H_2O$ incorporation rates were then converted to milligrams of cholesterol synthesized so that the rates of whole-animal cholesterol synthesis in D represent the milligrams of sterol newly synthesized per day per kilogram body weight. The asterisk (*) identifies those values in the knockout animals that were significantly different ($P < 0.05$) from the respective values seen in the control *Galgt1*$^{+/+}$/*Siat9*$^{+/+}$ mice. Each column represents the mean ± SEM.

triacylglycerol was marginally lower in the *Galgt1*$^{-/-}$/*Siat9*$^{-/-}$ mice (Fig. 2B).

### Cholesterol concentrations and synthesis rates in *Galgt1*$^{-/-}$/*Siat9*$^{+/+}$ mice

As seen in **Fig. 3A**, the organ weights in the animals lacking GM2/GD2 synthase were essentially the same as in the control mice, except for minor differences in the adrenal, kidney, and testis. Notably, both the absolute (Fig. 3A) and relative weights of the liver (5.58 ± 0.14 vs. 5.56 ± 0.08% of body weight) and brain (1.94 ± 0.07 vs. 1.87 ± 0.05%) were not significantly different in the *Galgt1*$^{-/-}$/*Siat9*$^{+/+}$ mice, compared with the control animals. Most important, the concentration of cholesterol in these organs was also nearly the same (Fig. 3B). Only the testis had a slightly higher sterol concentration (3.7 ± 0.1 vs. 2.3 ± 0.1 mg/g). As would be anticipated from prior reports, the highest concentrations of cholesterol were in the adrenal, where large amounts of cholesteryl esters are stored, and the CNS, where the sterol is entirely unesterified. The remaining organs had much lower concentrations of cholesterol, also nearly all unesterified, ranging from ~6 mg/g in the lung to ~1.0 mg/g in muscle. When these values were multiplied by the respective organ weights and summed, the whole-animal cholesterol pool in the *Galgt1*$^{-/-}$/*Siat9*$^{+/+}$ mice equaled 2,116 ± 14 mg/kg body weight, a value not significantly different from the value of 2,104 ± 18 mg/kg found in the *Galgt1*$^{+/+}$/*Siat9*$^{+/+}$ controls (Fig. 2C).

Deletion of GM2/GD2 synthase activity also did not alter rates of cholesterol synthesis in any organ except for small but significant differences in the colon and testis (Fig. 3C). When these rates of synthesis were multiplied by the respective organ weights and summed, the whole-animal cholesterol synthesis rate equaled 195 ± 6 mg/day/kg body weight in the *Galgt1*$^{-/-}$/*Siat9*$^{+/+}$ mice compared with a value of 208 ± 17 mg/day/kg in the control animals (Fig. 2D). Because the input of cholesterol into these animals from the diet was very small (<16 mg/day/kg), the rates of cholesterol turnover in the whole animal could be approximated from these synthesis data. The *Galgt1*$^{+/+}$/*Siat9*$^{+/+}$ control mice replaced about 9.8 ± 0.2% of their whole-body pool each day, whereas the *Galgt1*$^{-/-}$/*Siat9*$^{+/+}$ mice turned over about 9.2 ± 0.3% of their pool each day.

### Cholesterol concentrations and synthesis rates in *Galgt1*$^{+/+}$/*Siat9*$^{-/-}$ mice

As seen in Fig. 3A, the organ weights in animals lacking GM3 synthase were also essentially identical to those seen in the control animals. Furthermore, the weights relative

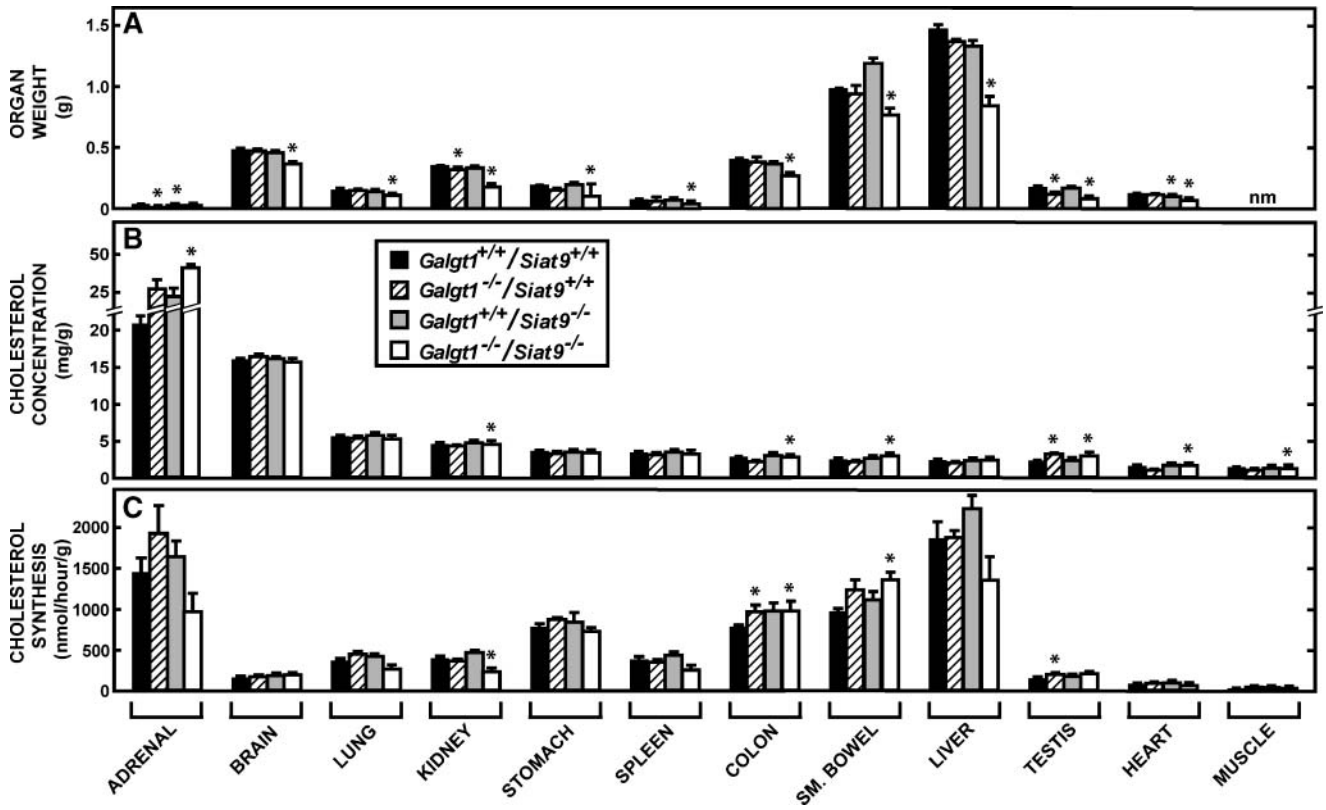


**Fig. 3.** Organ weights, cholesterol concentrations, and cholesterol synthesis rates in control mice and in animals lacking GM2/GD2 synthase, GM3 synthase, or both GM2/GD2 and GM3 synthase. Male *Galgt1*$^{+/+}$/*Siat9*$^{+/+}$ (n = 11), *Galgt1*$^{-/-}$/*Siat9*$^{+/+}$ (n = 6), *Galgt1*$^{+/+}$/*Siat9*$^{-/-}$ (n = 10), and *Galgt1*$^{-/-}$/*Siat9*$^{-/-}$ (n = 6) mice were euthanized at 49 days of age and whole-organ weights (A), tissue cholesterol concentrations (B), and rates of cholesterol synthesis (C) were measured. Cholesterol concentrations are expressed as milligrams of cholesterol per gram wet weight of tissue, and the synthesis rates are expressed as nanomoles of $^3H_2O$ incorporated into sterols per hour per gram of tissue. The asterisk (*) identifies those values in these three groups of mice that were significantly different ($P < 0.05$) from the respective values in the control *Galgt1*$^{+/+}$/*Siat9*$^{+/+}$ animals. Each column represents the mean ± SEM. nm, not measured.

to body mass of the liver (5.32 ± 0.19%) and brain (2.06 ± 0.05%) were not different from those found in the *Galgt1*$^{+/+}$/*Siat9*$^{+/+}$ animals. The concentration of cholesterol in every organ (Fig. 3B) also was identical to the respective values found in the control animals. Importantly, the mean concentration of cholesterol in the whole CNS in both the *Galgt1*$^{-/-}$/*Siat9*$^{+/+}$ (15.84 ± 0.25 mg/g) and *Galgt1*$^{+/+}$/*Siat9*$^{-/-}$ (16.19 ± 0.25 mg/g) mice was not significantly different from the value found in the *Galgt1*$^{+/+}$/*Siat9*$^{+/+}$ (16.07 ± 0.21 mg/g) animals. From these values, the whole-animal cholesterol pool was calculated to equal 2,155 ± 30 mg/kg in the mice lacking GM3 synthase activity (Fig. 2C). The rates of cholesterol synthesis in each of these organs also were not altered by loss of this enzymatic activity (Fig. 3C). From these latter values, the rate of whole-animal cholesterol synthesis was determined to equal 247 ± 6 mg/day/kg (Fig. 2D), and the rate of whole-animal cholesterol turnover equaled 11.0 ± 0.7%/day. Thus, there were virtually no significant alterations in any of these parameters of sterol metabolism in either the GM2/GD2 or GM3 knockout animals.

### Cholesterol concentrations and synthesis rates in *Galgt1*$^{-/-}$/*Siat9*$^{-/-}$ mice

These various parameters, however, were different in several respects in the *Galgt1*$^{-/-}$/*Siat9*$^{-/-}$ double-knockout mice. Both the whole-animal body weights (Fig. 2A) and the individual organ weights (Fig. 3D) were significantly lower than those found in the control mice. Although the profile of cholesterol concentrations in these organs was similar to that seen in the *Galgt1*$^{+/+}$/*Siat9*$^{+/+}$ mice (Fig. 3B), in the kidney, colon, small bowel, testis, heart, and striated muscle, there were slight but significant elevations in these concentrations (Fig. 3B). Several of these same organs, including kidney, colon, and small bowel, had slightly elevated rates of cholesterol synthesis (Fig. 3C). The whole-animal cholesterol pool was marginally elevated in the *Galgt1*$^{-/-}$/*Siat9*$^{-/-}$ animals (2,380 ± 35 mg/kg), compared with the *Galgt1*$^{+/+}$/*Siat9*$^{+/+}$ mice (2,104 ± 18 mg/kg) (Fig. 2C), whereas the rate of whole-animal cholesterol synthesis was essentially unchanged (218 ± 14 vs. 208 ± 17 mg/day/kg) (Fig. 2D). Importantly, from these values, the rate of turnover of the whole-animal sterol pool in the *Galgt1*$^{-/-}$/*Siat9*$^{-/-}$ mice equaled 9.1 ± 0.3%/day, a value essentially equal to that found in the control mice (9.8 ± 0.2%/day).

### Cholesterol concentrations and synthesis rates in regions of the CNS

Although there was no difference in the mean concentration of cholesterol in the whole CNS in these four groups of animals, it was still possible that there were regional differences in sterol metabolism in the brain that reflected loss of the GM2/GD2 and GM3 synthases. This possibility was explored in additional groups of animals, as illustrated in **Fig. 4**. As is evident, however, the concentration of cholesterol in the cerebrum, cerebellum, midbrain, brain stem, and spinal cord was virtually identical in the presence or absence of the GM2/GD2 or GM3 syn-

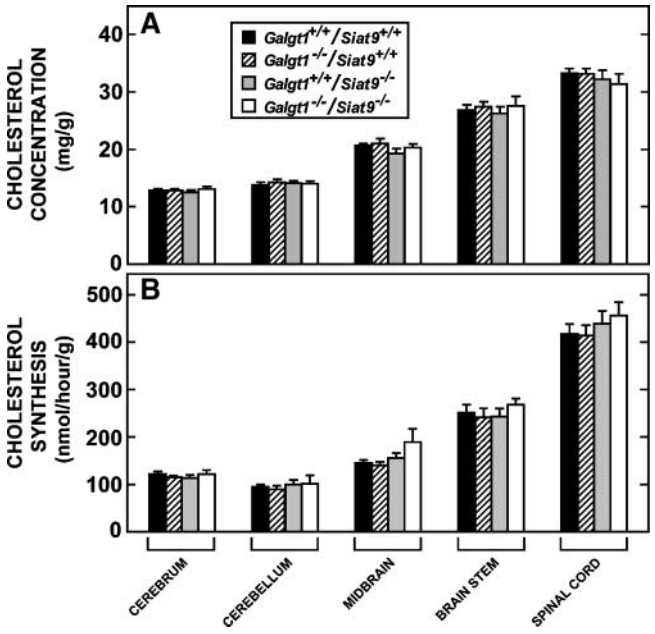


**Fig. 4.** Cholesterol concentrations and rates of cholesterol synthesis in different regions of the brain. The central nervous system of 49 day-old male animals with the four different genotypes (n = 10–15 in each group) was dissected into five regions. The overall concentrations of cholesterol (A) and rates of cholesterol synthesis (B) in each whole-brain region were determined. Each column represents the mean ± SEM, and there were no significant differences ($P > 0.05$) among the tissues from the different genotypes.

thases (Fig. 4A). There also were no significant differences in the rate of sterol synthesis in these same regions of the CNS in the *Galgt1*$^{-/-}$/*Siat9*$^{+/+}$, *Galgt1*$^{+/+}$/*Siat9*$^{-/-}$, or *Galgt1*$^{-/-}$/*Siat9*$^{-/-}$ mice (Fig. 4B). Furthermore, loss of these synthases did not alter the rates of cholesterol turnover in these regions of the CNS, which, in all groups of animals, averaged about 0.72%/day in the cerebrum, 0.53%/day in the cerebellum, 0.53%/day in the midbrain, 0.72%/day in the brain stem, and 0.96%/day in the spinal cord.

### Effect of cholesterol loading in animals lacking GM2/GD2 and GM3 synthase

A final study of the single-knockout mice evaluated whether these gangliosides might play a role in the disposition of exogenous cholesterol entering the body carried in chylomicron remnants. In the control *Galgt1*$^{+/+}$/*Siat9*$^{+/+}$ mice, cholesterol feeding from weaning resulted in a small but significant increase in the plasma cholesterol level, but not the plasma triacylglycerol level (**Fig. 5A**) and an increase in the concentration of cholesterol in the small bowel and liver (Fig. 5C). No other tissue, including the brain, manifested an increase in tissue cholesterol concentration in response to dietary cholesterol feeding (Fig. 5C, D). Virtually identical findings were observed in the *Galgt1*$^{-/-}$/*Siat9*$^{+/+}$ and *Galgt1*$^{+/+}$/*Siat9*$^{-/-}$ animals, in that both the intestine and liver had similar increases in cholesterol following cholesterol loading, whereas the concentration in the other organs remained unchanged. The exception to this was the adrenal, which did exhibit a small

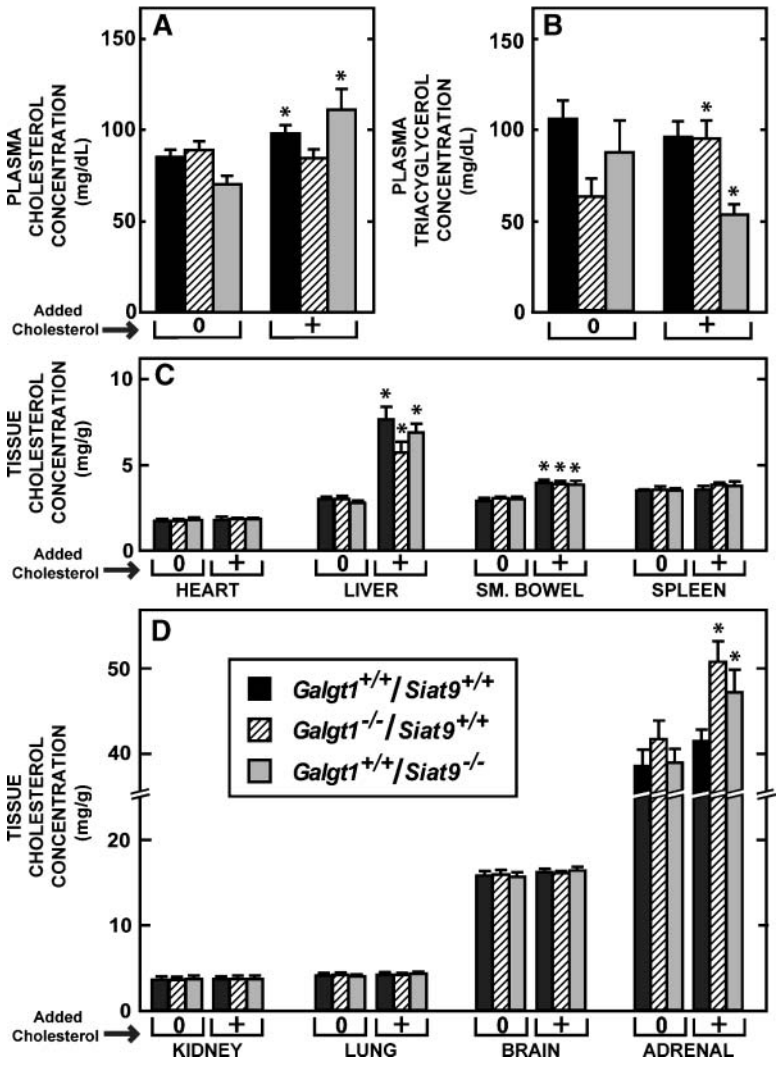


**Fig. 5.** Effect of cholesterol feeding on plasma and tissue cholesterol concentrations in female animals lacking GM2/GD2 or GM3 synthase activity. Groups of *Galgt1*$^{+/+}$/*Siat9*$^{+/+}$ (n = 12 in the low-cholesterol group and 8 in the cholesterol-fed group), *Galgt1*$^{-/-}$/*Siat9*$^{+/+}$ (n = 8 and 7, respectively), and *Galgt1*$^{+/+}$/*Siat9*$^{-/-}$ (n = 6 and 7, respectively) mice were fed either the low-cholesterol (0.02%) diet or this same diet with added cholesterol (1.0%, "+") beginning at weaning and continuing until 49 days of age, when the animals were euthanized. A, B: Plasma cholesterol and triacylglycerol concentrations, respectively, in these six groups of animals. C, D: Tissue cholesterol concentrations in the various organs in these respective groups. The asterisk (*) indicates those values in the cholesterol-fed animals that were different ($P < 0.05$) from the respective values in the mice fed the low-cholesterol diet. Each column represents the mean ± SEM of the values in each group.

but significant increase in cholesterol concentration in both groups of animals (Fig. 5D). Thus, expansion of the cholesteryl ester pool in the intestine and liver known to occur with cholesterol feeding took place normally in the absence of these two groups of gangliosides.

### Age at death of *npc1*$^{-/-}$ mice lacking specific gangliosides

Although these initial studies did not identify a role for either the GM2/GD2 or GM3 gangliosides in determining steady-state cholesterol balance in the tissues of the normal mouse, the next experiments investigated whether these same gangliosides might influence the amount of sterol trapped in the late endosomal/lysosomal compartment in the organs of mice carrying the *npc1* mutation. Deletion of GM2/GD2 synthase in the *npc1*$^{-/-}$ mouse has previously been reported to not change the clinical phenotype of this disease but did shorten the average age at death from 79 days in the *npc1*$^{-/-}$/*Galgt1*$^{+/+}$ animals to 69 days in the *npc1*$^{-/-}$/*Galgt1*$^{-/-}$ mice (33). The next experiment extended these observations to the *npc1*$^{-/-}$ mouse lacking GM3 synthase. As shown in **Fig. 6A**, the *npc1*$^{-/-}$/*Siat9*$^{+/+}$ and *npc1*$^{-/-}$/*Siat9*$^{-/-}$ animals performed equally poorly on the rotarod apparatus, compared with the control *npc1*$^{+/+}$/*Siat9*$^{+/+}$ mice. However, a second group of 36 *npc1*$^{-/-}$/*Siat9*$^{-/-}$ mice died at an average age of 64 days (Fig. 6B), which was significantly earlier than the average age at death, 85 days, seen in the *npc1*$^{-/-}$/*Siat9*$^{+/+}$ mice. Thus, as already reported in the *npc1*$^{-/-}$/*Galgt*$^{-/-}$ mice, deletion of GM3 synthase also did not alter the clinical phenotype of the *npc1*$^{-/-}$ mouse but did shorten its lifespan.

### Cholesterol concentration and synthesis rates in *npc1*$^{-/-}$ mice lacking GM2/GD2 or GM3 synthase

In the *npc1*$^{-/-}$ mouse, it was conceivable that these gangliosides normally reaching the late endosomal/lysosomal compartment during endocytosis could interact with sterols and lead to changes in cholesterol content and/or synthesis in the presence of the *npc1* mutation. Such differences, if present, could conceivably account for the protective effect of these gangliosides on the age at death of the mutant animals (Fig. 6B) (33). As illustrated in **Figs. 7B** and **8B**, respectively, the *npc1*$^{-/-}$/*Galgt1*$^{+/+}$ and *npc1*$^{-/-}$/*Siat9*$^{+/+}$ mice had the expected marked increases in cholesterol concentration in nearly every organ. This increase varied from about 1.4-fold in cardiac and striated muscle to over 8-fold in the liver. These differences presumably

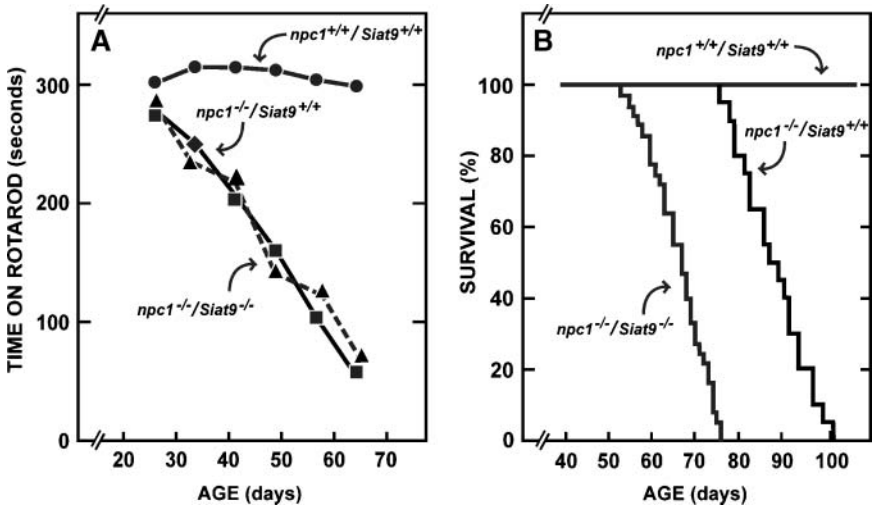


**Fig. 6.** Performance on the rotarod and age at death of $npc1^{-/-}$ mice either with or without GM3 synthase activity. Groups of $npc1^{+/+}/Siat9^{+/+}$ (n = 11), $npc1^{-/-}/Siat9^{+/+}$ (n = 7), and $npc1^{-/-}/Siat9^{-/-}$ (n = 19) mice containing both males and females were tested weekly on the rotarod apparatus, and the times they remained on the rotarod are shown in A. Additional groups of $npc1^{+/+}/Siat9^{+/+}$ (n = 10), $npc1^{-/-}/Siat9^{+/+}$ (n = 20), and $npc1^{-/-}/Siat9^{-/-}$ (n = 36) animals were followed until death (B). Although there was no difference in performance on the rotarod, the $npc1^{-/-}/Siat9^{-/-}$ animals died significantly ($P < 0.05$) earlier than the $npc1^{-/-}/Siat9^{+/+}$ mice.

reflected the varied rates of lipoprotein uptake through receptor-mediated and bulk-phase endocytosis in these different organs (5, 34). Only brain showed the small but significant reduction in cholesterol concentration previously reported (21). Even though neurons and glia accumulate unesterified cholesterol in NPC disease (35, 36), this small reduction in sterol content in the CNS presumably reflects the partial demyelination that accompanies the neurodegeneration taking place in the presence of this mutation.

Deletion of either GM2/GD2 or GM3 synthase in the $npc1^{-/-}$ mice resulted in marginally, though not significantly, lower body weights and, in a few instances, smaller organ weights (Figs. 7A, 8A). However, the elevated levels of cholesterol seen in the $npc1^{-/-}$ animals were unaltered in most organs of these double-knockout mice (Figs. 7B, 8B). In particular, the marked increase in hepatic cholesterol levels and the small reduction in brain sterol concentrations found in the $npc1^{-/-}$ mice were unchanged when the activity of either synthase was deleted. Because of these increases in cholesterol content in nearly all organs, the whole-animal cholesterol pools increased from about 2,100 mg/kg in the $npc1^{+/+}/Galgt1^{+/+}$ and $npc1^{+/+}/Siat9^{+/+}$ control mice to over 5,000 mg/kg in the $npc1^{-/-}$ animals, regardless of whether the *Galgt1* or *Siat9* genes were expressed.

In many organs of the $npc1^{-/-}$ mice, there were also increases in the rate of cholesterol synthesis, as has been previously described (21). Such increases were usually seen in lung, kidney, and various parts of the gastrointestinal tract, and were similar regardless of whether GM2/GD2 (Fig. 7C) or GM3 (Fig. 8C) synthase activity was deleted. Thus, in these 49 day-old $npc1^{-/-}$ mice, the sequestration of an additional 3,000 mg/kg of cholesterol in the late endosomal/lysosomal compartments of the cells of all organs was unaffected by whether these compartments also contained gangliosides of the GM2/GD2 or GM3 series.

### Hepatic and cerebellar disease in the presence and absence of NPC1 and GM3 synthase function

Because loss of GM3 synthase function clearly shortened the lifespan of the $npc1^{-/-}$ mice (Fig. 6B), a final series of studies examined whether this protein might play a role in determining the severity of the specific organ dysfunctions seen in the $npc1^{-/-}$ mice. The liver is a major target of this mutation, and the degree of hepatocellular death has been shown to be proportional to the amount of unesterified cholesterol that accumulates in macrophages and hepatocytes (5, 24). As seen in **Fig. 9**, in both the $npc1^{+/+}/Siat9^{+/+}$ and $npc1^{+/+}/Siat9^{-/-}$ animals, relative liver weight, cholesterol concentration, and various liver function tests were all within normal limits. In contrast, deletion of NPC1 function led to enlargement of the liver, a marked increase in cholesterol concentration, and abnormal liver function tests. Deletion of GM3 synthase activity, however, in the $npc1^{-/-}$ mouse had little or no significant effect on the amount of sterol in the liver or on the abnormal liver function tests. Although not shown, identical findings were observed in the $npc1^{-/-}/Galgt1^{-/-}$ mice (n = 7). Thus, deletion of either the GM2/GD2 or GM3 synthase did not alter the severity of the liver disease seen in the $npc1^{-/-}$ mice.

The Purkinje cells of the cerebellum are another major target of this mutation and are reported to be largely destroyed by 49 days of age (37). As was true in the liver, deletion of GM3 synthase activity in the $npc1^{+/+}$ mice had no effect on the relative mRNA levels of various proteins in the cerebellum (Fig. 9F). However, as previously reported (26), loss of NPC1 function markedly increased the mRNA levels of MIP1a and GFAP, proteins associated with glial ac-

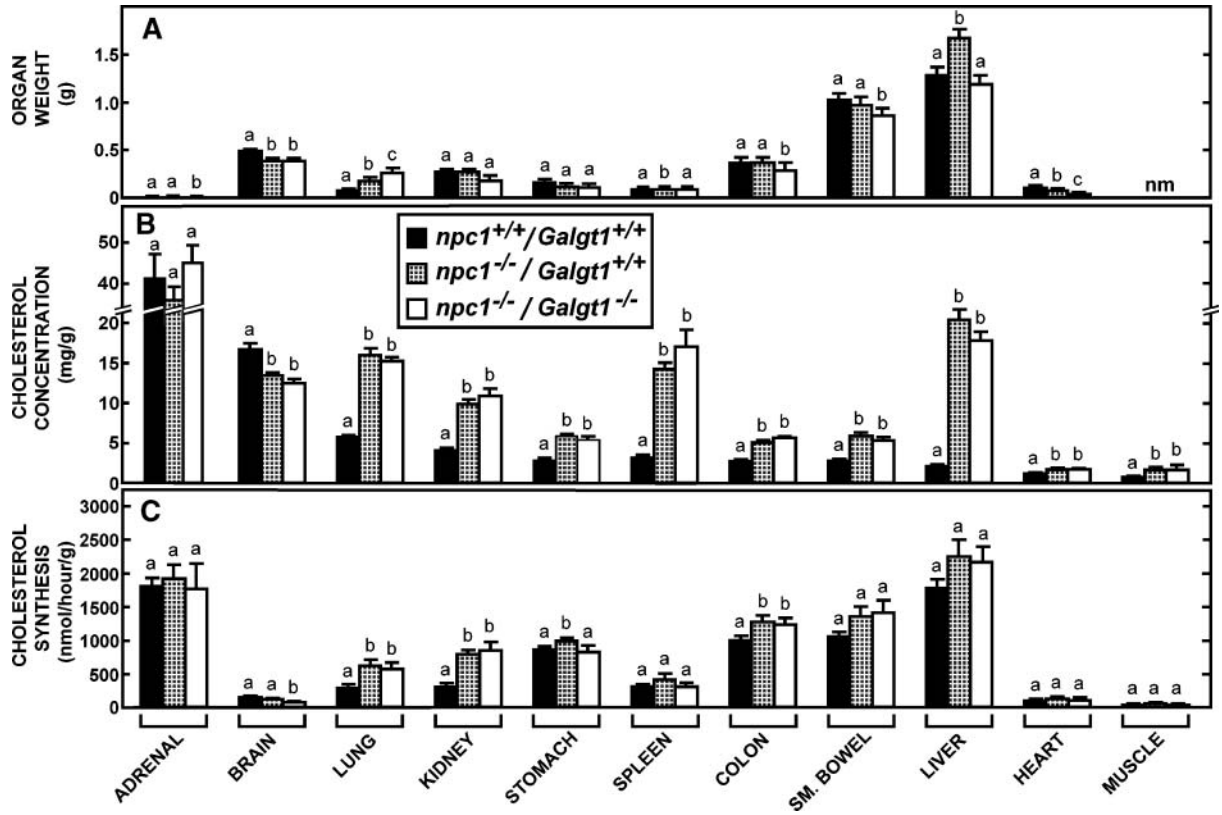


**Fig. 7.** Organ weights, cholesterol concentrations, and cholesterol synthesis rates in mice lacking NPC1 function in the presence or absence of GM2/GD2 synthase activity. Groups of $npc1^{+/+}/Galgt1^{+/+}$ (n = 7), $npc1^{-/-}/Galgt1^{+/+}$ (n = 8), and $npc1^{-/-}/Galgt1^{-/-}$ (n = 6) mice, including both males and females, were maintained on the low-cholesterol diet and studied at 49 days of age. A: Organ weights in these animals. The concentration of cholesterol and the rates of cholesterol synthesis in these organs are shown in B and C, respectively. Significant differences ($P < 0.05$) in the groups are designated by different letters. Each column represents the mean ± SEM. nm, not measured.

tivation, and APOE, Casp1, and Casp3, proteins that reflect nerve cell damage. In contrast, the levels of PCP2, which reflects Purkinje cell number, and MBP, which reflects myelin synthesis, were reduced or unchanged. Importantly, elimination of GM3 synthase activity in the $npc1^{-/-}/Siat9^{-/-}$ mice did not consistently make worse or improve these indirect measures of cerebellar disease. Thus, although deletion of GM3 synthase activity in the $npc1^{-/-}$ mouse significantly shortened the lifespan of these animals, it did not alter the severity of either the hepatic or cerebellar disease, at least as measured by these parameters.

## DISCUSSION

Unesterified cholesterol accounts for about one-fifth of the lipid molecules making up the plasma membrane of cells throughout the body and it plays a critical role in determining both the fluidity and permeability of this membrane. The concentration of sterol in the intracellular membranes of the endoplasmic reticulum, golgi, and mitochondria is much lower, so that most of the cholesterol in the cell, >90% in some studies (38, 39), resides in the plasma membrane. As a consequence, in the normal animal, the steady-state content of cholesterol in most tissues is primarily determined by the amount of unesterified sterol present in the plasma membrane of the cells making up each organ. In the mouse, for example, these values vary from about 5 mg/g wet weight in tissues like the lung and kidney to approximately 1 mg/g in striated muscle (Figs. 3, 7, 8). The exceptions to this generalization are the CNS and endocrine organs. In the brain, there is a second, large pool of unesterified cholesterol present in the compact myelin surrounding the axons of neurons. Thus, the total concentration of sterol in the CNS is much higher than in other tissues, averaging about 16 mg/g (Figs. 3, 7, 8), and this value varies regionally from about 13 mg/g in the cerebrum to over 30 mg/g in the heavily myelinated spinal cord (Fig. 4). Because about 80% of this sterol is in myelin, in the whole brain, only approximately 3 mg/g of the total of 16 mg/g represents unesterified cholesterol in the plasma membranes of neurons and glial cells (40). The endocrine glands are the second exception, and in the adrenal, for example, where the concentration of plasma membrane unesterified cholesterol is about 5 mg/g (41), there is a second pool of sterol exceeding 20 mg/g, made up of cholesteryl esters stored in lipid droplets in the cytosol (Figs. 3, 7, 8). Thus, in the CNS and adrenal, changes in the tissue total cholesterol levels may not necessarily reflect changes in plasma membrane cholesterol.

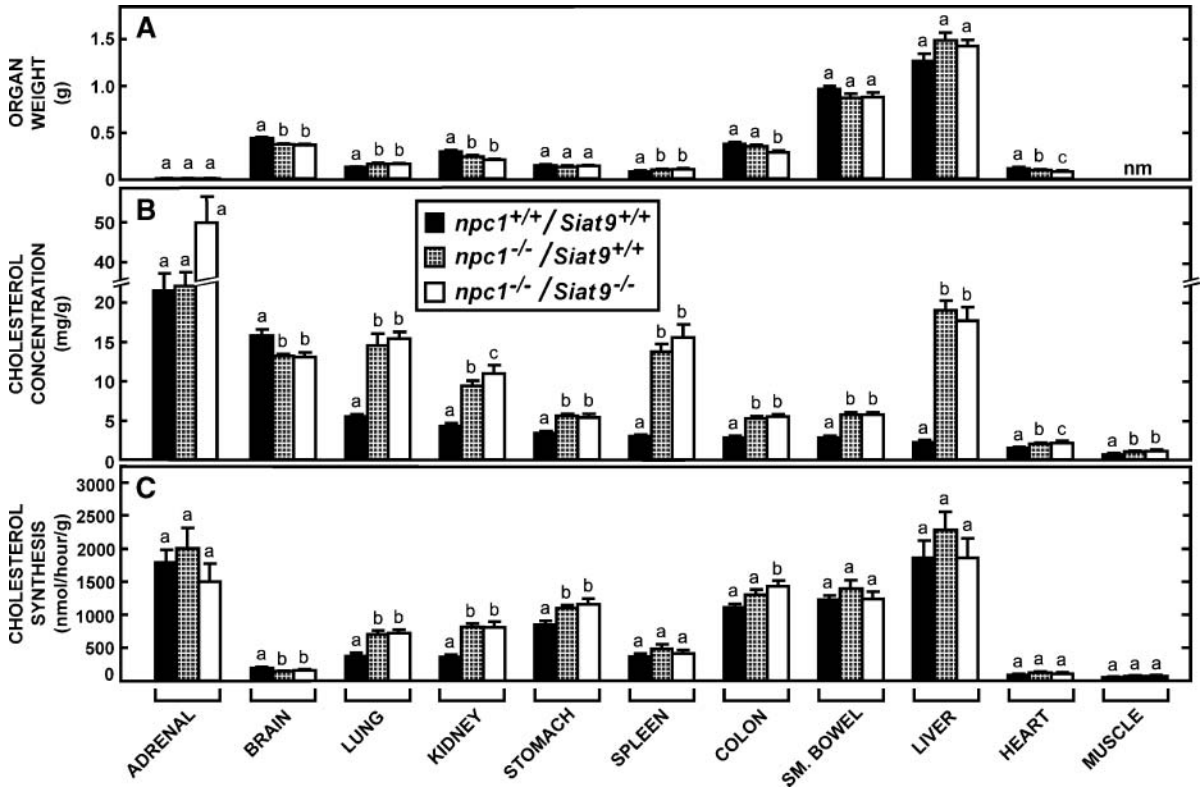


**Fig. 8.** Organ weights, cholesterol concentrations, and cholesterol synthesis rates in mice lacking NPC1 function in the presence and absence of GM3 synthase activity. Groups of $npc1^{+/+}/Siat9^{+/+}$ (n = 11), $npc1^{-/-}/Siat9^{+/+}$ (n = 10), and $npc1^{-/-}/Siat9^{-/-}$ (n = 8) mice, both males and females, were maintained on the low-cholesterol diet and studied at 49 days of age. A: Organ weights in these animals. The concentration of cholesterol and the rates of cholesterol synthesis in these organs are illustrated in B and C, respectively. Significant differences ($P < 0.05$) in the groups are designated by the different letters. Each column represents the mean ± SEM. nm, not measured.

Nevertheless, these studies provide strong evidence that the various gangliosides present in the plasma membrane do not play a significant role in sterol homeostasis in most organs or in the whole animal. In animals lacking either GM2/GD2 or GM3 synthase, early development was indistinguishable from that in control mice, whole-animal body and organ weights at 49 days of age were normal (Figs. 2A, 3A), and the steady-state concentration of cholesterol in virtually every tissue was unchanged (Fig. 3B). Although it was still conceivable that tissue sterol turnover through the plasma membrane was affected by ganglioside deletion, this also proved not to be the case, in that cholesterol synthesis was unaltered in nearly all organs (Fig. 3C), so that whole-animal turnover was essentially the same in the $Galgt1^{+/+}/Siat9^{+/+}$ (9.8%/day), $Galgt1^{-/-}/Siat9^{+/+}$ (9.2%/day), and $Galgt1^{+/+}/Siat9^{-/-}$ (11.0%/day) animals. In particular, it is important to note that deletion of either of these synthases did not significantly alter the weights (Fig. 3A), cholesterol concentrations (Fig. 4A), or sterol turnover rates in any region of the CNS, implying that in both of these knockout mouse strains, cholesterol homeostasis in the cellular plasma membranes and in myelin was unaltered in the brain, as in the other organs.

Even more remarkable were the findings in the $Galgt1^{-/-}/Siat9^{-/-}$ animals that lacked virtually all complex gangliosides. These mice did exhibit poor early development and weight gain (Fig. 2A); however, for the most part, the concentration of cholesterol and the rates of synthesis in the various tissues were similar to those found in the wild-type littermates (Fig. 3). There were small but significant increases in the cholesterol levels in organs like the colon, small bowel, testis, and muscle, and several of these same organs showed small increases in synthesis. Importantly, however, both the cholesterol concentration and synthesis rates were unaltered in all regions of the brain (Fig. 4). These latter findings are particularly noteworthy, given the fact that the brain normally has relatively high concentrations of the GM1, GD1a, GD1b, and GT1b gangliosides (Fig. 1), as well as lesser amounts of the other intermediates (19, 42). However, even though these complex gangliosides were absent from the CNS in these double-knockout mice, these animals could still synthesize galactosylceramide and the sulfated product of this glycolipid (SM4) (Fig. 1), both of which are major lipid components of myelin. In general, the level of myelin present in the brain is directly proportional to the amount of these galactolipids found in the CNS (43). Thus, the fact that the concentration and rates of turnover of cholesterol in the various regions of the CNS were normal (Fig. 4) probably reflects the fact that sterol homeostasis in both the cellular elements and myelin was unaffected, even by the total absence of these major gangliosides.

Potential interactions between gangliosides and cholesterol that normally occur within the plasma membrane

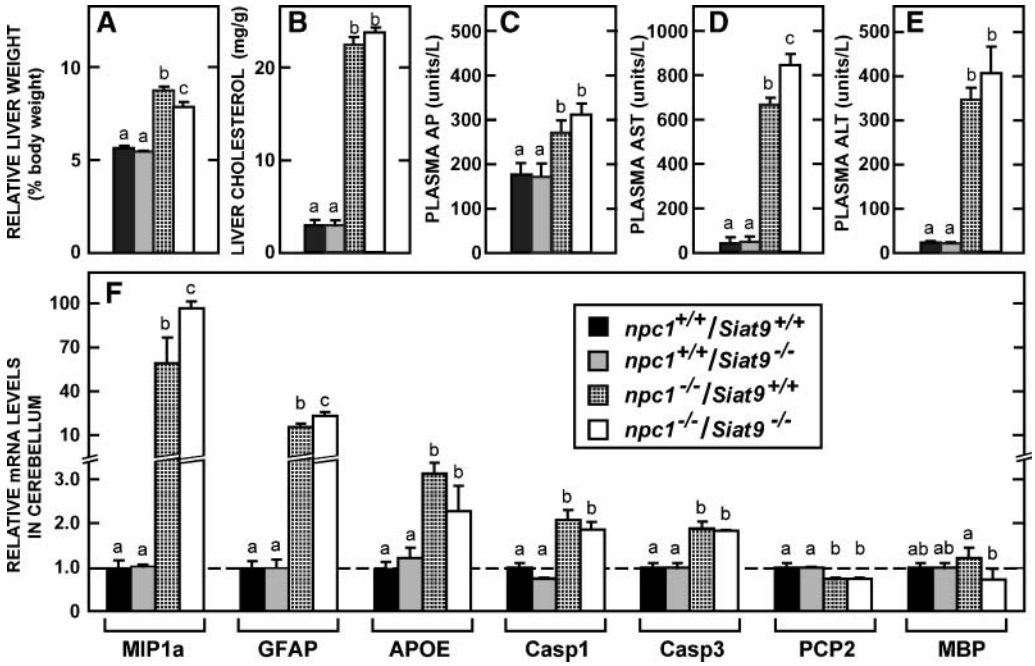


**Fig. 9.** Liver function tests and cerebellar mRNA levels in mice lacking NPC1 function in the presence and absence of GM3 synthase. Groups of $npc1^{+/+}/Siat9^{+/+}$ (n = 6), $npc1^{-/-}/Siat9^{+/+}$ (n = 6), and $npc1^{-/-}/Siat9^{-/-}$ (n = 6) mice, both males and females, were maintained on the low-cholesterol diet and studied at 49 days of age. A–E: Relative liver weights and liver cholesterol concentrations as well as various liver function tests, including the plasma alkaline phosphatase (AP), plasma aspartate aminotransferase (AST), and plasma alanine aminotransferase (ALT) activities. F: Relative mRNA levels in the cerebellum for a number of different proteins. Significant differences ($P < 0.05$) in the groups are designated by different letters. Each column represents the mean ± SEM.

may become more extensive in other regions of the cell in NPC1 disease. Nearly all cells take up sterol carried in lipoproteins through both receptor-mediated and bulk-phase endocytosis utilizing clathrin-coated pits (5). As these particles reach the late endosomal/lysosomal compartment of the cell, the cholesteryl ester carried in the lipoproteins is hydrolyzed and the unesterified cholesterol is transported, through the action of NPC1 protein, to the metabolically active pool of sterol within the cytosolic compartment. When the *npc1* gene is mutated, this unesterified cholesterol accumulates within the late endosomal/lysosomal compartment of cells throughout the body. Because this expanded pool of sterol is not "sensed" by the regulatory mechanisms in the endoplasmic reticulum and nucleus, uptake of lipoprotein cholesterol continues unabated throughout life and the rate of cholesterol synthesis actually increases (34). Hence, by 49 days of age, the concentration of unesterified cholesterol is elevated and synthesis is increased in nearly every organ of the $npc1^{-/-}$ mouse (Figs. 7, 8). As a result, the whole-animal cholesterol pool expands from about 2,100 mg/kg, most of which is in plasma membranes, to approximately 5,000 mg/kg, a large part of which is trapped within the late endosomal/lysosomal compartment of cells (21, 36, 44).

It is likely that this trapped cholesterol does interact with gangliosides in some manner, so as to cause a simultaneous sequestration of these complex glycolipids. In NPC1 disease, in both the human and the mouse, there is abnormal accumulation of gangliosides in cells of the CNS as well as in fibroblasts (15, 33, 45, 46). Whether this accumulation reflects primarily hydrophobic interactions between the cholesterol and ganglioside molecules or is the result of the more general endosomal/lysosomal dysfunction known to exist in NPC1 and other lysosomal storage diseases remains to be elucidated (47–49). In either case, however, it is clear that the reverse situation is not true, i.e., the abnormal accumulation of cholesterol within cells is not dependent upon ganglioside accumulation. The concentration of unesterified cholesterol and the rate of cholesterol synthesis in the tissues of the $npc1^{-/-}$ mouse were essentially unaffected by the presence or absence of functional GM2/GD2 or GM3 synthase (Fig. 7). These findings are consistent with the view that NPC1 protein does function primarily to move unesterified cholesterol from the late endosomal/lysosomal compartment to the metabolically active pool of sterol in the cytosol.

Further, these findings are also consistent with the thesis that the clinical disease manifest in specific organs of individuals with the NPC1 mutation is, in some manner, correlated with the amount of cholesterol that accumulates in the cells of these particular tissues. The liver, for example, accumulates large amounts of unesterified cholesterol (Figs. 7, 8) and manifests severe liver function abnormalities (Fig. 9) (50). Although elimination of gangliosides does not alter this disease (Fig. 9), treatment with drugs that block cholesterol absorption and lower receptor-mediated

sterol uptake into the liver brings about a reduction in the concentration of unesterified cholesterol in hepatocytes and does significantly improve liver function (24). Similarly, although deletion of either GM2/GD2 or GM3 synthase activity does not improve the measures of cerebellar dysfunction (Fig. 9) or prolong the lifespan (Fig. 6) of the *npc1*$^{-/-}$ mouse, treatment with an LXR agonist that increases cholesterol loss from the brain and reduces cellular sterol content does improve these measures of cerebellar disease and does prolong survival (37, 51). Taken together, therefore, these findings also strongly suggest that in the NPC1 syndrome, it is the accumulation of unesterified cholesterol within cells, and not gangliosides, that initiates cell death and, ultimately, clinical disease.

However, this is not to say that loss of the various gangliosides does not affect the integrity of specific organs or the overall health of the animal. In mice that are otherwise genetically intact, deletion of either the GM2/GD2 or GM3 synthase causes changes in neural conduction velocity and sensitivity to insulin (18, 32). Animals lacking both synthases have poor early development, axonal degeneration, and multiple histological abnormalities of the CNS (17, 19). Inactivation of either of these synthases in mice lacking NPC1 function shortens the mean life expectancy of these mutant animals (Fig. 6) (33). Clearly, then, gangliosides located in the plasma membrane have important cellular functions that are currently only partially understood. Nevertheless, the current studies strongly imply that unesterified cholesterol, another important component of the plasma membrane, is regulated and metabolized in a manner that is entirely independent of the metabolism of these complex gangliosides.

The authors thank Heather Waddell and S. Sean Campbell for their excellent technical assistance and Kerry Foreman for expert preparation of the manuscript. They also thank Dr. Richard L. Proia at the National Institutes of Health for providing the breeding stock of the *Galgt1*$^{-/-}$ and *Siat9*$^{-/-}$ mice and for critically reviewing this manuscript.

## REFERENCES

1. Dietschy, J. M., S. D. Turley, and D. K. Spady. 1993. Role of liver in the maintenance of cholesterol and low density lipoprotein homeostasis in different animal species, including humans. *J. Lipid Res.* **34:** 1637–1659.
2. Osono, Y., L. A. Woollett, J. Herz, and J. M. Dietschy. 1995. Role of the low density lipoprotein receptor in the flux of cholesterol through the plasma and across the tissues of the mouse. *J. Clin. Invest.* **95:** 1124–1132.
3. Brown, M. S., and J. L. Goldstein. 1979. Receptor-mediated endocytosis: insights from the lipoprotein receptor system. *Proc. Natl. Acad. Sci. USA.* **76:** 3330–3337.
4. Innerarity, T. L., and R. W. Mahley. 1978. Enhanced binding by cultured human fibroblasts of apo-E-containing lipoproteins as compared with low density lipoproteins. *Biochemistry.* **17:** 1440–1447.
5. Liu, B., C. Xie, J. A. Richardson, S. D. Turley, and J. M. Dietschy. 2007. Receptor-mediated and bulk-phase endocytosis cause macrophage and cholesterol accumulation in Niemann-Pick C disease. *J. Lipid Res.* **48:** 1710–1723.
6. Dietschy, J. M., and S. D. Turley. 2002. Control of cholesterol turnover in the mouse. *J. Biol. Chem.* **277:** 3801–3804.
7. Simons, K., and E. Ikonen. 2000. How cells handle cholesterol. *Science.* **290:** 1721–1726.
8. Smaby, J. M., M. Momsen, V. S. Kulkarni, and R. E. Brown. 1996. Cholesterol-induced interfacial area condensations of galactosylceramides and sphingomyelins with identical acyl chains. *Biochemistry.* **35:** 5696–5704.
9. Hakomori Si, S. I. 2002. The glycosynapse. *Proc. Natl. Acad. Sci. USA.* **99:** 225–232.
10. Kolter, T., R. L. Proia, and K. Sandhoff. 2002. Combinatorial ganglioside biosynthesis. *J. Biol. Chem.* **277:** 25859–25862.
11. Slotte, J. P., and E. L. Bierman. 1988. Depletion of plasma-membrane sphingomyelin rapidly alters the distribution of cholesterol between plasma membranes and intracellular cholesterol pools in cultured fibroblasts. *Biochem. J.* **250:** 653–658.
12. Scheek, S., M. S. Brown, and J. L. Goldstein. 1997. Sphingomyelin depletion in cultured cells blocks proteolysis of sterol regulatory element binding proteins at site 1. *Proc. Natl. Acad. Sci. USA.* **94:** 11179–11183.
13. Glaros, E. N., W. S. Kim, C. M. Quinn, J. Wong, I. Gelissen, W. Jessup, and B. Garner. 2005. Glycosphingolipid accumulation inhibits cholesterol efflux via the ABCA1/apolipoprotein A-I pathway. *J. Biol. Chem.* **280:** 24515–24523.
14. te Vruchte, D., E. Lloyd-Evans, R. J. Veldman, D. C. A. Neville, R. A. Dwek, F. M. Platt, W. J. van Blitterswijk, and D. J. Sillence. 2004. Accumulation of glycosphingolipids in Niemann-Pick C disease disrupts endosomal transport. *J. Biol. Chem.* **279:** 26167–26175.
15. Gondré-Lewis, M. C., R. McGlynn, and S. U. Walkley. 2003. Cholesterol accumulation in NPC1-deficient neurons is ganglioside dependent. *Curr. Biol.* **13:** 1324–1329.
16. Riboni, L., P. Viani, R. Bassi, A. Prinetti, and G. Tettamanti. 1997. The role of sphingolipids in the process of signal transduction. *Prog. Lipid Res.* **36:** 153–195.
17. Sheikh, K. A., J. Sun, Y. Liu, H. Kawai, T. O. Crawford, R. L. Proia, J. W. Griffin, and R. L. Schnaar. 1999. Mice lacking complex gangliosides develop Wallerian degeneration and myelination defects. *Proc. Natl. Acad. Sci. USA.* **96:** 7532–7537.
18. Yamashita, T., A. Hashiramoto, M. Haluzik, H. Mizukami, S. Beck, A. Norton, M. Kono, S. Tsuji, J. L. Daniotti, N. Werth, et al. 2003. Enhanced insulin sensitivity in mice lacking ganglioside GM3. *Proc. Natl. Acad. Sci. USA.* **100:** 3445–3449.
19. Yamashita, T., Y-P. Wu, R. Sandhoff, N. Werth, H. Mizukami, J. M. Ellis, J. L. Dupree, R. Geyer, K. Sandhoff, and R. L. Proia. 2005. Interruption of ganglioside synthesis produces central nervous system degeneration and altered axon-glial interactions. *Proc. Natl. Acad. Sci. USA.* **102:** 2725–2730.
20. Loftus, S. K., J. A. Morris, E. D. Carstea, J. Z. Gu, C. Cummings, A. Brown, J. Ellison, K. Ohno, M. A. Rosenfeld, D. A. Tagle, et al. 1997. Murine model of Niemann-Pick C disease: mutation in a cholesterol homeostasis gene. *Science.* **277:** 232–235.
21. Xie, C., S. D. Turley, P. G. Pentchev, and J. M. Dietschy. 1999. Cholesterol balance and metabolism in mice with loss of function of Niemann-Pick C protein. *Am. J. Physiol.* **276:** E336–E344.
22. Liu, Y., A. Hoffmann, A. Grinberg, H. Westphal, M. P. McDonald, K. M. Miller, J. N. Crawley, K. Sandhoff, K. Suzuki, and R. L. Proia. 1997. Mouse model of $G_{M2}$ activator deficiency manifests cerebellar pathology and motor impairment. *Proc. Natl. Acad. Sci. USA.* **94:** 8138–8143.
23. Repa, J. J., S. D. Turley, G. Quan, and J. M. Dietschy. 2005. Delineation of molecular changes in intrahepatic cholesterol metabolism resulting from diminished cholesterol absorption. *J. Lipid Res.* **46:** 779–789.
24. Beltroy, E. P., B. Liu, J. M. Dietschy, and S. D. Turley. 2007. Lysosomal unesterified cholesterol content correlates with liver cell death in murine Niemann-Pick type C disease. *J. Lipid Res.* **48:** 869–881.
25. Schwarz, M., D. W. Russell, J. M. Dietschy, and S. D. Turley. 1998. Marked reduction in bile acid synthesis in cholesterol 7α-hydroxylase-deficient mice does not lead to diminished tissue cholesterol turnover or to hypercholesterolemia. *J. Lipid Res.* **39:** 1833–1843.
26. Li, H., J. J. Repa, M. A. Valasek, E. P. Beltroy, S. D. Turley, D. C. German, and J. M. Dietschy. 2005. Molecular, anatomical, and biochemical events associated with neurodegeneration in mice with Niemann-Pick type C disease. *J. Neuropathol. Exp. Neurol.* **64:** 323–333.
27. Kurrasch, D. M., J. Huang, T. M. Wilkie, and J. J. Repa. 2004. Quantitative real-time polymerase chain reaction measurement of regulators of G-protein signaling mRNA levels in mouse tissues. *Methods Enzymol.* **389:** 3–15.

28. Valasek, M. A., and J. J. Repa. 2005. The power of real-time PCR. *Adv. Physiol. Educ.* **29:** 151–159.
29. Turley, S. D., J. M. Andersen, and J. M. Dietschy. 1981. Rates of sterol synthesis and uptake in the major organs of the rat in vivo. *J. Lipid Res.* **22:** 551–569.
30. Dietschy, J. M., and D. K. Spady. 1984. Measurement of rates of cholesterol synthesis using tritiated water. *J. Lipid Res.* **25:** 1469–1476.
31. Xie, C., S. D. Turley, and J. M. Dietschy. 2000. Centripetal cholesterol flow from the extrahepatic organs through the liver is normal in mice with mutated Niemann-Pick type C protein (NPC1). *J. Lipid Res.* **41:** 1278–1289.
32. Takamiya, K., A. Yamamoto, K. Furukawa, S. Yamashiro, M. Shin, M. Okada, S. Fukumoto, M. Haraguchi, N. Takeda, K. Fujimura, et al. 1996. Mice with disrupted GM2/GD2 synthase gene lack complex gangliosides but exhibit only subtle defects in their nervous system. *Proc. Natl. Acad. Sci. USA.* **93:** 10662–10667.
33. Liu, Y., Y-P. Wu, R. Wada, E. B. Neufeld, K. A. Mullin, A. C. Howard, P. G. Pentchev, M. T. Vanier, K. Suzuki, and R. L. Proia. 2000. Alleviation of neuronal ganglioside storage does not improve the clinical course of the Niemann-Pick C disease mouse. *Hum. Mol. Genet.* **9:** 1087–1092.
34. Xie, C., S. D. Turley, and J. M. Dietschy. 1999. Cholesterol accumulation in tissues of the Niemann-Pick type C mouse is determined by the rate of lipoprotein-cholesterol uptake through the coated-pit pathway in each organ. *Proc. Natl. Acad. Sci. USA.* **96:** 11992–11997.
35. Xie, C., D. K. Burns, S. D. Turley, and J. M. Dietschy. 2000. Cholesterol is sequestered in the brains of mice with Niemann-Pick type C disease but turnover is increased. *J. Neuropathol. Exp. Neurol.* **59:** 1106–1117.
36. Reid, P. C., N. Sakashita, S. Sugii, Y. Ohno-Iwashita, Y. Shimada, W. F. Hickey, and T-Y. Chang. 2004. A novel cholesterol stain reveals early neuronal cholesterol accumulation in the Niemann-Pick type C1 mouse brain. *J. Lipid Res.* **45:** 582–591.
37. Repa, J. J., H. Li, T. C. Frank-Cannon, M. A. Valasek, S. D. Turley, M. G. Tansey, and J. M. Dietschy. 2007. LXR activation enhances cholesterol loss from the brain, decreases neuroinflammation and increases survival of the NPC1 mouse. *J. Neurosci.* **27:** 14470–14480.
38. Slotte, J. P., G. Hedström, S. Rannström, and S. Ekman. 1989. Effects of sphingomyelin degradation on cell cholesterol oxidizability and steady-state distribution between the cell surface and the cell interior. *Biochim. Biophys. Acta.* **985:** 90–96.
39. Lange, Y. 1992. Tracking cell cholesterol with cholesterol oxidase. *J. Lipid Res.* **33:** 315–321.
40. Dietschy, J. M., and S. D. Turley. 2004. Cholesterol metabolism in the central nervous system during early development and in the mature animal. *J. Lipid Res.* **45:** 1375–1397.
41. Xie, C., J. A. Richardson, S. D. Turley, and J. M. Dietschy. 2006. Cholesterol substrate pools and steroid hormone levels are normal in the face of mutational inactivation of NPC1 protein. *J. Lipid Res.* **47:** 953–963.
42. Svennerholm, L., K. Boström, B. Jungbjer, and L. Olsson. 1994. Membrane lipids of adult human brain: lipid composition of frontal and temporal lobe in subjects of age 20 to 100 years. *J. Neurochem.* **63:** 1802–1811.
43. Morell, P., and R. H. Quarles. 1999. Myelin formation, structure and biochemistry. *In* Basic Neurochemistry. Molecular, Cellular and Medical Aspects. G. J. Siegel, B. W. Agranoff, R. W. Albers, S. K. Fisher, and M. D. Uhler, editors. Lippincott-Raven, Philadelphia, PA. 78.
44. Blanchette-Mackie, E. J. 2000. Intracellular cholesterol trafficking: role of the NPC1 protein. *Biochim. Biophys. Acta.* **1486:** 171–183.
45. Vanier, M. T. 1999. Lipid changes in Niemann-Pick disease type C brain: personal experience and review of the literature. *Neurochem. Res.* **24:** 481–489.
46. Watanabe, Y., S. Akaboshi, G. Ishida, T. Takeshima, T. Yano, M. Taniguchi, K. Ohno, and K. Nakashima. 1998. Increased levels of $GM_2$ ganglioside in fibroblasts from a patient with juvenile Niemann-Pick disease type C. *Brain Dev.* **20:** 95–97.
47. Zhang, M., N. K. Dwyer, D. C. Love, A. Cooney, M. Comly, E. Neufeld, P. G. Pentchev, E. J. Blanchette-Mackie, and J. A. Hanover. 2001. Cessation of rapid late endosomal tubulovesicular trafficking in Niemann-Pick type C1 disease. *Proc. Natl. Acad. Sci. USA.* **98:** 4466–4471.
48. Zhang, M., N. K. Dwyer, E. B. Neufeld, D. C. Love, A. Cooney, M. Comly, S. Patel, H. Watari, J. F. Strauss III, P. G. Pentchev, et al. 2001. Sterol-modulated glycolipid sorting occurs in Niemann-Pick C1 late endosomes. *J. Biol. Chem.* **276:** 3417–3425.
49. Liao, G., Y. Yao, J. Liu, Z. Yu, S. Cheung, A. Xie, X. Liang, and X. Bi. 2007. Cholesterol accumulation is associated with lysosomal dysfunction and autophagic stress in $Npc1^{-/-}$ mouse brain. *Am. J. Pathol.* **171:** 962–975.
50. Beltroy, E. P., J. A. Richardson, J. D. Horton, S. D. Turley, and J. M. Dietschy. 2005. Cholesterol accumulation and liver cell death in mice with Niemann-Pick type C disease. *Hepatology.* **42:** 886–893.
51. Langmade, S. J., S. E. Gale, A. Frolov, I. Mohri, K. Suzuki, S. H. Mellon, S. U. Walkley, D. F. Covey, J. E. Schaffer, and D. S. Ory. 2006. Pregnane X receptor (PXR) activation: a mechanism for neuroprotection in a mouse model of Niemann-Pick C disease. *Proc. Natl. Acad. Sci. USA.* **103:** 13807–13812.